Gamma Radiation Synthesis of Colloidal Silver Nanoparticles

EDUARD MARIUS LUNGULESCU[1], GABRIELA SBARCEA[1]*, RADU SETNESCU[1,2], NICOLETA NICULA[1], ROBERT DUCU[1], ANA MARIA LUPU (LUCHIAN)[1], IOANA ION[1], VIRGIL MARINESCU[1]

[1]National R&D Institute for Electrical Engineering (ICPE-CA), 313 Splaiul Unirii, 030138, Bucharest, Romania

[2]Valahia University of Targoviste, Faculty of Sciences and Arts, 2 Carol I Str., 130024, Targoviste, Romania

Radiochemical synthesis of metallic nanoparticles is an eco-friendly method allowing the obtaining of controlled size, well dispersed and highly stable particles at very mild conditions. Colloidal silver nanoparticles were synthesized in a one-step process, in an aqueous system consisting of polyvinyl alcohol (PVA)/Ag^+/ isopropyl alcohol (IPA), irradiated at various doses by using high energy ionizing radiations (γ-rays). The UV-Vis spectra have shown a maximum absorption peak in the range of 390-450 nm, specific for silver nanoparticles. The size of the obtained spherical shape nanoparticles was below 50 nm and decreased with increasing of the irradiation dose.

Keywords : metal nanoparticles, gamma irradiation, antimicrobial, silver nanoparticles

The current applications of ionizing radiation and their connection with nanotechnology represent a research area that has gained special attention in recent years [1-4]. The revolutionary development of science and engineering has enabled the synthesis of nano-sized materials in order to take advantage of their unique properties that differ significantly from those of the individual atoms [5, 6].

The nanoscale particles of transitional metals have unique physical and chemical properties that allow them to be used in a wide range of possible applications such as information storage, optoelectronics, sensors, renewable energy technologies and catalysts, medical imaging, biocidal or antimicrobial agents, etc. [7-15]. A number of factors such as size, dimensional distribution and particle shape have a major influence on the functional properties of these materials [16]. Consequently, there is an increased interest in the development of methods enabling better controlled synthesis of the nanoparticles [17]. Silver/ polymer based nanostructures are studied intensively due to their potential applications in electronics [18], optical devices [19], catalysis [20], biosensors [21], antibacterial medical devices [22] and in biomedical applications (wounds, tissue scaffolds, antimicrobial filters) towing to their antibacterial properties [23].

Silver nanoparticles are also used in the antimicrobial applications such as fungal, viruses and bacteria annihilation [24], obtaining of water filtration membranes with biocide activity against the microorganisms present in water [25] etc. The action of Ag nanoparticles on the biological systems depends on properties such as surface chemistry, size and shape, size distribution, morphology, particle composition and reactivity, agglomeration and dissolution rate, the efficiency of ions release and the type of reducing agents used for their synthesis [26]. The bioavailability of the therapeutic agents that are administered systemically and locally is enhanced by the physicochemical properties of the used nanoparticles [27]. The development of Ag nanoparticles with uniform structures in terms of size, morphology and functionality are essential for biomedical applications, because Ag nanoparticles can influence cellular absorption, biological distribution, penetration into biological barriers and the resulting therapeutic effects [28-30].

In this paper, colloidal solutions of silver nanoparticles were obtained by gamma ionizing radiation, starting from precursor systems containing silver ions (silver nitrate solution) stabilized with polyvinyl alcohol (PVA) in the presence of isopropyl alcohol. The effects of the irradiation dose on the ultimate characteristics of the radiation-synthesized silver nanoparticles, such as the average size, shape and antimicrobial properties, were studied.

Experimenmtal part

Materials

The materials used in the present work were silver nitrate as precursor (Chemical Company, Rumania), polyvinyl alcohol (M_w = 89000-98000, Sigma Aldrich) acting as a stabilizer of silver nanoparticles, isopropyl alcohol (IPA Chimreactiv SRL, Rumania) as radical $OH^\bullet$ scavenger and deionized water as solvent. All reagents were used as received, without further purifications.

Preparation of aqueous PVA/$AgNO_3$ solution

The solution of PVA (6% m / v) was prepared under magnetic stirring at 98°C until a clear polymer solution was obtained. Then, an amount of $AgNO_3$ corresponding to a concentration of 1 mM was added into solution. The obtained solution was homogenized under magnetic stirring at 70° C for 1 h, and the *p*H was kept constant at 8-9 by adding drops of NaOH solution. The solution was bubbled with N_2 for 30 min for deaeration. Isopropyl alcohol was added to obtain a 20% v/v mixture with the PVA / Ag nitrate solution.

Irradiation

The PVA/Ag^+/IPA solutions sealed in glass containers were exposed to γ-irradiation in an Ob-Servo Sanguis installation (Institute of Isotopes, Hungary), equipped with ^{60}Co source, at room temperature and atmospheric pressure. Radiation doses ranged from 0 to 100 kGy at a dose rate of 1.2 kGy / h.

Characterization of silver nanoparticles

UV-Vis Spectroscopy (Jasco V-570, JP) was performed in the spectral range of 300-800 nm, in PS vials of 1 cm, with a resolution of 1 nm, on colloidal solutions diluted with ultrapure water (4:6 v/v). Aqueous solution of PVA (6%) was used as reference.

Infrared Spectroscopy (Jasco FTIR-4200, JP) was carried out in the spectral range of 400-4000 cm^{-1} with a resolution of 4 cm^{-1} and 50 scans /spectrum. For measurements, the colloidal nanoparticle solutions or the

* email: gabriela.sbarcea@icpe-ca.ro

initial polymer solution were coated in a thin layer on a ZnSe window and the spectral acquisition was made in transmission mode.

The hydrodynamic diameter and particles size distribution were measured on diluted aqueous suspensions by *Dynamic Light Scattering (DLS)* technique using a 90 Plus nanoparticle size analyzer (Brookhaven Instruments Corporation) equipped with 35 mW solid-state laser with 660 nm wavelength. DLS measurements were performed at a scattering angle of 90° and a temperature of 25°C.

X-ray diffraction (XRD-Bruker-AXS type D8 DISCOVER) measurements were performed using the following parameters: X-ray tube with Cu anode, 40 kV / 40 mA; increment: 0.04 °; scanning rate: 1s; measuring range 2 θ = 10 ° - 100 °. The identification was performed using the database from International Center of Diffraction Data (ICDD).

All *scanning electron microscopy* images were recorded with an FE-SEM model Auriga, Carl Zeiss, Germany involving in chamber secondary electron detector In-Lens annular type, with an accelerating voltage of 5 kV on non-coated samples.

The antimicrobial tests were performed according to the following procedure: the exposure to a fungi suspension (a mixture of *Aspergillus niger, Aspergillus terreus, Aureobasidium pullulans, Penicillium funiculosum, Penicillium ochrochloron, Paecilomyces variotii, Scopulariopsis brevicaulis, Trichoderma viride, Chaetomium globosum*) was performed on complete Czapek-Dox culture media poured in Petri dishes, according to SR EN 60068-2-10 [31]. Fungal growth was observed at regular intervals of 3, 7, 14 and 21 days;

The bacterial inoculum was represented by *Staphylococcus sp.* grown on LB agar (10 g peptone, 5 g yeast extract, 5 g NaCl, 12 g agar), with a cellular density corresponding to 0.5 McFarland turbidity standard (150x106 CFU/mL). The volume of the colloidal silver nanoparticles solution used was 100 µL/well.

Results and discussions

The radiochemical synthesis principle of metallic nanoparticles is based on the radiolysis of the aqueous solutions meaning transfers of a high amount of energy to the irradiated material, with several orders of magnitude higher than the average energy required to break any chemical bond; this energy transfer is non-selective.

The interaction of γ-radiation with aqueous solutions leads to the generation of free electrons by photoelectric absorption and Compton scattering, as well as to the production of primary species of water radiolysis such as hydrated electrons (e_{aq}^-), hydrogen radicals, hydroxyl radicals, etc. [32].

$$H_2O \xrightarrow{\gamma} e_{aq}^-, H_3O^+, H^\bullet, H_2, OH^\bullet, H_2O_2 \quad (1)$$

Hydrated electrons and hydrogen radicals (H atoms) are strongly reducing species and can reduce Ag^+ ions to Ag metal (eq. (2)). The Ag^0 atoms may interact with Ag^+ ions by forming relatively stable clusters of silver (eq. (3)) [33]. Silver nanoparticles are formed either by combining these clusters or by absorbing a neutral Ag^0 atom.

$$Ag^+ + e_{aq}^- \xrightarrow{\text{reduction}} Ag^0 \quad (2)$$

$$Ag^0 + Ag^+ \rightarrow Ag_2^+$$
$$Ag^+ + Ag_2^+ \rightarrow Ag_3^+ \quad (3)$$

On the other hand, hydroxyl radicals ($OH^\bullet$) resulting from the water radiolysis process have the ability to oxidize either ions or atoms to higher oxidation states. Therefore, in order to prevent this process, OH× radical scavengers such as isopropyl alcohol are used [34].

UV-Vis Spectroscopy

A first indication of silver nanoparticle formation is given by color change of irradiated PVA / Ag^+ / IPA solutions: they gradually darken from transparent-colorless to yellow and then brown (fig. 1).

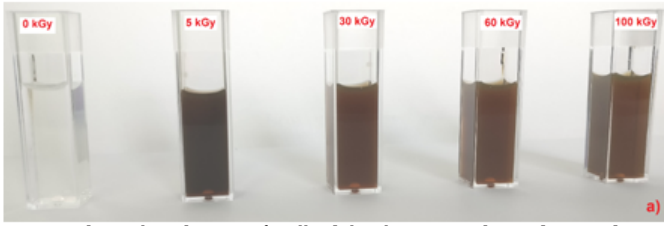

Fig.1.The color change of colloidal solutions with irradiation dose: PVA/Ag^+/IPA;

In order to confirm the formation of silver nanoparticles, UV-Vis absorption spectra of irradiated colloidal solutions were recorded. Figure 2 shows the UV-Vis spectra of colloidal silver nanoparticles. The optical absorption spectra of colloidal solutions of Ag nanoparticles is dominated by the SPR (Surface Plasmon Resonance) band [34]. Generally, silver nanoparticles show the specific SPR band with peaks between 390 and 500 nm.

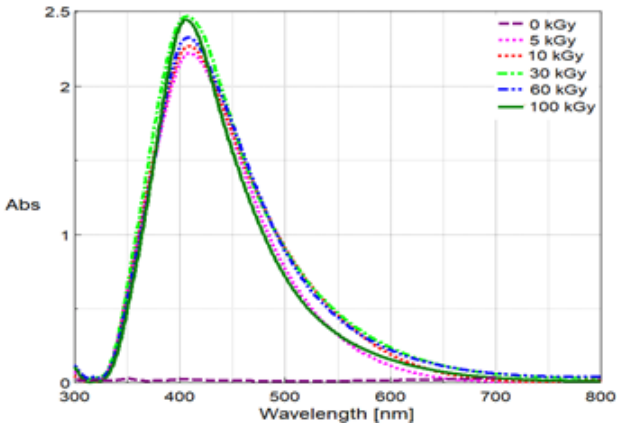

Fig.2. UV-Vis spectra recorded for PVA / Ag+ / IPA colloidal system. Solutions diluted with deionized water: 4:6 (v/v)

Table 1 summarizes the characteristic parameters of the SPR band for the analyzed samples. It can be seen that SPR maximum is slightly shifted to shorter wavelengths, and FWHM parameter decreases as the irradiation dose increased. The position and the shape of SPR band is dependent on both particles size and solution concentration [34, 35]. SPR band moves to lower wavelengths with decreasing the average size of nanoparticles [36], and the height of this band increases as increasing the nanoparticles concentration. The FWHM parameter (full

Table 1
THE PARAMETERS OF SPR BAND

Dose (kGy)	Position of maximum SPR (nm)	Absorbance* (u.a.)	FWHM (nm)
5	410	2.20	112.3
30	407	2.43	110.2
60	408	2.29	112.4
100	405	2.43	96.8

* Dilution with deionized water: 4/6 (v/v)

width at half maximum) is correlated to the dispersion degree of nanoparticle dimensions: a high value of FWHM is associated with a large polydispersity [36]. Thus, it can be concluded that higher doses result in lower particle size and narrower dimensional distribution.

This behavior can be explained in terms of density of nucleation event: at high doses, the nucleation events are more present than the number of ions, radiation synthesis produces small nanoparticles and the process is followed by their aggregation. At low doses, when nucleation events are lower than the total number of ions, the metal nanoparticles have large dimensions [34].

On the other hand, a secondary reduction step induced by gamma radiation would be the intermolecular and intramolecular crosslinking processes between the polymer molecules, based on free radicals mechanism. Hence, at higher irradiation doses, the structure of the polymer matrix will be complex as a result of both formation of intermolecular and intramolecular hydrogen bonds, and radiation-crosslinking between the cyclic PVP molecules [37]. Thus, the coalescence of metallic nanoparticles is prevented, resulting the formation of smaller nanoparticles.

The stability tests carried-out on the silver nanoparticles colloidal solutions have evidenced their high stability even after a storage of 9 months in laboratory conditions; the visual examinations of the aqueous solutions did not present any deposits at the bottom of the glass containers and the SPR parameters obtained from UV-Vis spectra suffered slight modifications (fig. 3).

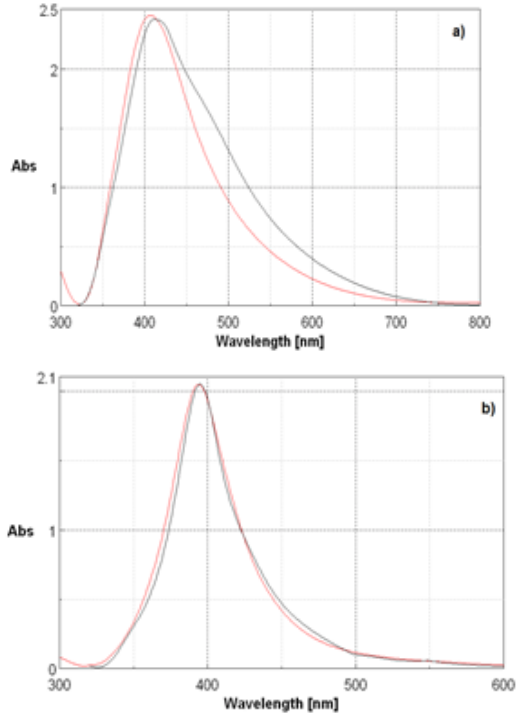

Fig.3. Influence of PVA concentration on the silver colloidal solutions stability (D=30 kGy): a) 80% PVA: initial (red); after 9 months (black); b) 1 % PVA: initial (red); after 9 months (black). Solutions diluted with deionized water: 4:6 (v/v)

It has been observed that the concentration of the polymer has a great influence on the stability of the colloidal nanoparticle system. Thus, for the colloidal solutions with high PVA amount (about 80 %) and irradiated at 30 kG it was observed a red shift of the SPR maximum of about 7 nm, a slight decrease of 0.3 a.u. of the SPR intensity and a larger FWHM, respectively, as compared to the initial solutions (fig. 3a). At lower PVA concentration (bellow 20%), the SPR parameters remain unmodified.

Taking into account this results we can conclude that radiation-synthesized silver nanoparticles present higher stability on long term.

Dynamic light scattering (DLS)

DLS measurements performed on the colloidal silver nanoparticles confirmed the results obtained by UV-Vis spectroscopy: the mean diameter (D_{mean}) decreases with the irradiation dose from 30 nm to about 20 nm.

Dose (kGy)	D_{mean} [nm]
5	**30**±0.010
30	**25**±0.089
60	**23**±0.050
100	**20**±0.024

D_{mean}- mean diameter

Table 2
THE VALUES OF MEAN DIAMETER DETERMINED BY DLS TECHNIQUE

X-ray Diffraction

The qualitative phase analysis by X-ray diffraction was used to determine the influence of the synthesis parameters on the crystalline structure of the radio-chemically synthesized Ag nanoparticles clusters. The analyzed samples present in XRD patterns four main peaks at 2 θ= 38.4°, 44,3°, 64.8°, 77.7° and a very small peak at 81.8° (fig. 4). Their reflexions are indexed with the planes (111), (200), (220), (311), and (222), that correspond to the cubic face centered (FCC) crystallographic structure of silver. The crystallite size was calculated using Scherrer formula: D= K λ/ β· cosθ, where λ is the wavelength of X-ray (0.1541 nm), K is the shape factor (0.9), β is FWHM (full width at half maximum), è represents the diffraction angle, and D is the crystallite size. An increase in the intensity of the peaks can be observed with the irradiation dose (fig.3).

All the analyzed samples present a shift of the peaks to larger angles, resulting in lower cell parameters (table 3). A 0.4085 nm value was obtained according to the PDF card ICDD).

Scanning Electronic Microscopy (SEM)

This technique was used in order to analyze the morphological structure of the silver nanoparticles and for the determination of their size and shape. Figure 5 shows the SEM images obtained on colloidal systems, irradiated at 30 kGy. As can be seen, the radiation-synthesized silver

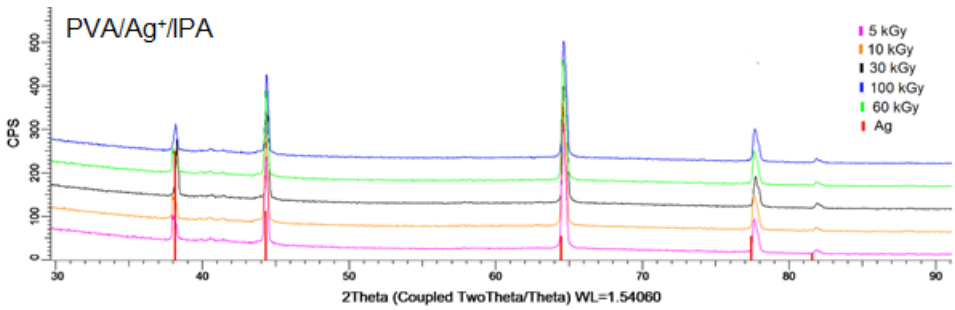

Fig. 4. XRD pattern obtained for PVA/Ag^+/IPA colloidal system

Table 3

CELL PARAMETERS OF PVA/AG$^+$/IPA COLLOIDAL SYSTEM

Dose (kGy)	Crystallographic phase	2θ [°]	Lattice parameters a=b=c [nm]	Crystallite size [nm]
5	Cubic Ag	38.4	0.4077	31.6
10		44.3	0.4077	31.6
30		64.8	0.4071	30.9
60		77.7	0.4075	31.9
100		81.8	0.4072	31.1

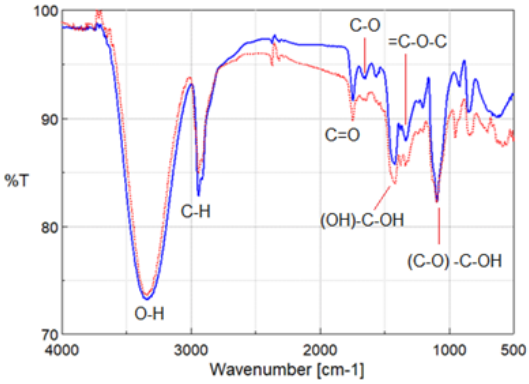

Fig. 6.Comparative FTIR spectra for PVA (without Ag, blue) and PVA/Ag$^+$ (red) samples; Irradiation dose of 60 kGy

nanoparticles present mainly a spherical shape with the average dimensions similar to those obtained by DLS technique and in agreement with the SPR maximum peaks obtained from UV-Vis spectra.

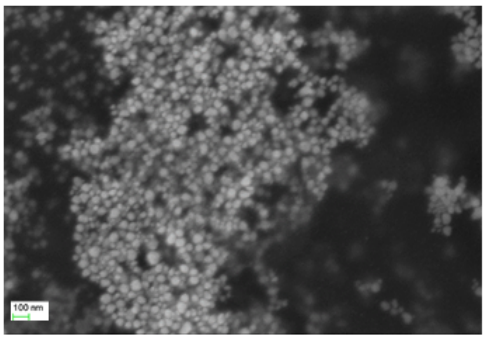

Fig. 5.SEM images recorded for PVA/Ag$^+$/IPA colloidal system irradiated at 30 kGy

Infrared Spectroscopy

FTIR spectroscopy was used to prove the ability of PVA to coat and stabilize the silver nanoparticles. Figure 6 shows the FTIR spectra recorded on the solutions of silver nanoparticles obtained in the presence of PVA, in comparison with the polymer solution without Ag nanoparticles. The formation of PVA-Ag bonds (due to the coating of Ag nanoparticles with PVA) produces changes in the PVA-Ag FTIR spectrum. Thus, it can be seen a decrease in the intensities of the bands corresponding to carbonyl or -OH active groups [38], i.e. 1745 cm^{-1} (C = O), or 1424 cm^{-1} [(OH) -C-OH] and 1096 cm^{-1}[(CO) -C-OH], respectively, that suggests the formation of chemical bonds between PVA and Ag. PVA polymer chain plays an important role in avoiding the formation of Ag nanoparticles clusters. PVA contains several active OH groups which are able to retain Ag ions by secondary reactions and sterical hindrance [39], according to the following reaction:

$$R\text{-}OH + Ag^+ \longrightarrow R\text{-}O\text{-}Ag + H^+ \quad (4)$$

In this case, R-OH represents the PVA monomer.

Antimicrobial proprieties

These properties were illustrated in figure 7. The exposure to both fungal and bacterial suspensions showed a local antimicrobial effect (fig. 7a). The sizes of the inhibition zones were between 20-26 mm (fig. 7b). The 100 kGy irradiated samples showed zones of inhibition comparable in size with those of the 5 kGy irradiated samples (approx. 21 mm) even though the silver nanoparticles are smaller in size. This is due to the physical barrier created by the polymer which prevents the diffusion of the nanoparticles in the growth media. The barrier is created by structural modification of the polymer due to irradiation in which intramolecular crosslinking processes take place. This phenomenon becomes apparent starting with 60 kGy and the polymer becomes visibly more viscous. The size of the inhibition zones created by the silver nanoparticles is comparable to the size of the inhibition zones created by commercial antibiotics [40], like oxacillin (≥22mm at 35µg), gentamicin (≥15mm at 10µg), kanamycin (≥18mm at 30µg), tobramycin (≥15mm at 10µg), azithromycin (≥18 mm at 15 µg) and erythromycin (≥23mm at 15µg). The fungi suspension showed a positive influence of the silver nanoparticles solutions. The solutions have an antifungal effect, with the maximum effect at 30 kGy. At higher doses, the efficiency is lower, probably due to the crosslinking of the polymer matrix.

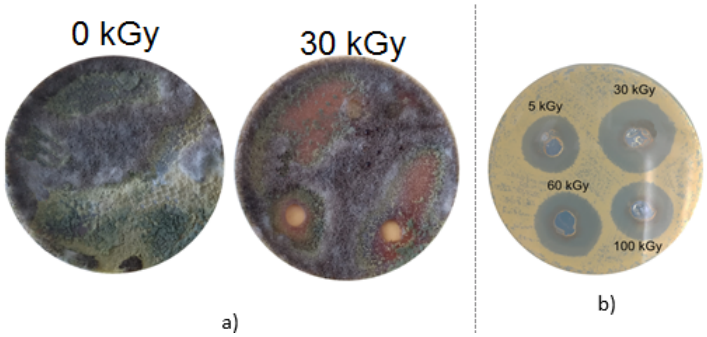

Fig. 7. The efficiency of silver nanoparticles solutions: fungi suspension (a, 30 kGy); growth inhibition of Staphylococcus sp. (b)

Table 4

INHIBITION ZONES FOR STAPHYLOCOCCUS SP

Dose (kGy)	Inhibition zone (mm) PVA/Ag$^+$/IPA
5	20
30	26
60	22
100	21

Conclusions

The experimental results have shown that the radiochemical synthesis is a simple and rapid method for obtaining controlled-size Ag nanoparticles, with good antimicrobial effectiveness.

The formation of radiation-induced Ag nanoparticles was visually confirmed by yellow-brown color of irradiated solutions, but also by the different analysis techniques, namely UV-Vis spectroscopy, XRD, DLS and SEM. The conclusions inferred from these measurements are perfectly convergent.

FTIR spectroscopy proved the coating ability of Ag nanoparticles by PVA component with the formation of chemical bonds between the polymer and silver nanoparticles. The polymer samples with Ag nanoparticles showed a decrease in the bands intensity of C = O groups (1745 cm^{-1}) and of some active -OH bands compared to the initial polymer;

Radiation-synthesized Ag nanoparticles exhibit local antifungal and antibacterial activity (*Staphylococcus sp.*) with an inhibition zone of 21-26 mm. The antibacterial activity is similar to that of some commercial antibiotics (according to Clinical and Laboratory Standard Institute: penicillin, oxacillin, kanamycin, erythromycin, etc.). The antimicrobial activity is influenced by the average size of the nanoparticles, but it would be also affected by crosslinking of the polymer matrix which can prevent nanoparticle diffusion into the specific culture medium.

Acknowledgments:The financial support was provided by Ministry of Research and Innovation, through PN 19310101-46N/2019, Grant No 04-4-1122-2015/2020 and contract 30PFE/2018 (between National R&D Institute for Electrical Engineering ICPE-CA and Romanian Ministry of Research and Innovation - MCI)

References

1. CHMIELEWSKI A.G., AL-SHEIKHLY M., BEREJKA A.J., CLELAND M.R., ANTONIAK M. ,Radiat. Phys. Chem. **94,** 2014, p.147-150
2. FARAHANI M., CLOCHARD M-C., GIFFORD I., BARKATT A., AL-SHEIKHLY M. Radiat. Phys. Chem. **105,** 2014, p.39 - 47
3. PASANPHAN W., RATTANAWONGWIBOON T., CHOOFONG S., GÜVEN O., KATTI K.K., Radiat. Phys. Chem., **106,** 2015, p. 360-370
4.POSTEK M.T., POSTER D.L., VLADAR A.E., DRISCOLL M.S., LAVERNE J.A., TSINAS Z., AL-SHEIKHLY M.I., Radiat. Phys. Chem. **143,** 2018, p. 47-52
5. WANG L., ZHANG Z., HAN X., NPG Asia Mater., **5**, 2013, p.40
6. MILLER J.C., SERRATO R.M., REPRESAS-CARDENAS J.M., KUNDAHL G.A. The Handbook of Nanotechnology. John Wiley & Sons, Inc., Hoboken, New Jersey, 2005
7. CAMPELO J.M., LUNA D., LUQUE R., MARINAS J.M., ROMERO A.A., ChemSusChem, **2**, 2009, p.18–45
8. CUENYA B.R., Thin Solid Films, **518**, 20103, p.127–3150
9. DATSYUK V., KALYVA M., PAPAGELIS K., PARTHENIOS, J., TASIS, D., SIOKOU, A., KALLITSIS, I., GALIOTIS, C., Carbon, **46**, 2008, p.833–840
10. DU C., AO Q., CAO N., YANG L., LUO W., CHENG G., Int. J. Hydrog. Energy, **40**, 2015, p.6180–6187
11. KAWASAKI, H., Nanotechnol. Rev., **2**, 2013
12. KUILA T., BOSE S., MISHRA, A.K. KHANRA, P. KIM, N.H. LEE J.H., Prog. Mater. Sci., **57**, 2012, p.1061–1105
13. MARQUARDT D., VOLLMER C., THOMANN R., STEURER P. MÜLHAUPT R. REDEL E. JANIAK C., Carbon, **49**, 2011, p.1326–1332
14. XU H., ZENG L., XING S., SHI G., XIAN Y., JIN L., Electrochem. Commun., **10**, 2008, p.1839-1843
15. GHAZI O.A., IBRAHIM M.M., ABOU ELFADL F.I., HOSNI H.M., SHEHATA E.M., DEGHIEDY N.M., BALBOUL M.R., J. Radiat. Research. Appl. Sci., **8**, 2015, p.166-172
16. GUISBIERS, G., ABUDUKELIMU, G., HOURLIER, D., Nanoscale Research Letters., **6**, 2011, p.396
17. HEI, H., Soft Nanoscience Letters., **2**, 2012, p.34-40
18. LI Y., WU Y., ONG B.S., J., Am. Chem. Soc., **127**, 2005 p.3266 –3267
19. MATSUDA S.I., YASUDA Y., ANDO S., Adv. Mater. **17**, 2005, p.2221-2224
20. AHMED K.B.A., J. Photochem. Photobiol. B Biol., **151**, 2015, p.39 - 45
21. LIU Y., WANG G., LI C., ZHOU Q., WANG M., YANG L., Mater. Sci. Eng., C **35**, 2014, p.253 –258
22. SON W.K., YOUK J.H., LEE T.S., PARK W.H., Macromol. Rapid Commun. **25**, 2004 p.1632 –1637
23. FERRARIA A.M., BOU S., BATTAGLINI N., BOTELHO DO REGO A.M., REIVILAR M., Langmuir, **26**, 2009, p.1996 –2001
24. MONTEIRO D.R., GORUP L.F., TAKAMIYA A.S., RUVOLLO-FILHO A.C., CAMARGO E.R.D., Int. J. Antimicrobial Agents, **34**, 2009, p.103-110
25. AHAMED M., ALSALHI M.S., SIDDIQUI M.K., Clin. Chim. Acta., **411,** 2010, p.1841-1848
26.CARLSON, C.; HUSSAIN, S.M.; SCHRAND, A.M.; BRAYDICH-STOLLE, L.K.; HESS, K.L.; JONES, R.L.; SCHLAGER, J.J., J. Phys. Chem. B, **112**, 2008, p.13608–13619
27. JO, D.H.; KIM, J.H.; LEE, T.G.; KIM, J.H., Nanomedicine, **11**, 2015, p.1603–1611
28. DUAN, X.P.; LI, Y.P., Small, **9**, 2013, p.1521–1532
29. SRIRAM, M.I.; KANTH, S.B.M.; KALISHWARALAL, K.; GURUNATHAN, S. Int. J. Nanomed., **5**, 2010, p.753–762
30. XI-FENG Z., ZHI-GUO L., WEI S., SANGILIYANDI G., Int. J. Medical Sciences, 2016
21.*** SR EN ISO 60068-2-10. Environmental testing -Part 2-10: Tests - Test J and guidance : Mould growth, 2010
32. BELLONI J., Catal. Today, 2006, **113**, p.141 –156
33. CHEN M., FENG Y.G., WANG X., LI T.C., ZHANG J.Y., Langmuir, **23**, 2007, p.5296-5304
34. NAGHAVI K., SAION E., REZAEE K., YUNUS W.M.M., Radiat. Phys. Chem., **79**, 2010, p.1203-1208
35. EGHBALIFAM N., FROUNCHI M., DADBIN., Int. J. Biol. Macromol., **80**, 2015, p.170-178
36 AGNIHOTRI S., MUKHERJI S., MUKHERJI S., RSC Adv., **4**, 2014, p.3974-3983
37. KASSAEE M., A. AKHAVAN, N. SHEIKH, R. BETESHOBABRUD., Radiat. Phys. Chem., **77**, 2008, p.1074–1078
38. ABEDINI A, DAUD A.R., HAMID M.A.A., OTHMAN N. K., SAION E., Nanoscale Research Letters, **8**, 2013, p.474-484
39. GAUTAM A., TRIPATHY P., RAM S., J. Mater. Sci., **41**, 2006, p.3007–3016
40. ***Clinical and Laboratory Standard Institute: M100-S24 Performance standards for antimicrobial susceptibility Testing; Twenty-fourth informational supplement, 2014

Manuscript received: 3.12.2018